

# Growth of SiGe/Si Quantum Well Structures by Atmospheric Pressure Chemical Vapor Deposition

D.A. GRÜTZMACHER, T.O. SEDGWICK, A. ZASLAVSKY, A.R. POWELL,  
R.A. KIEHL, W. ZIEGLER, and J. COTTE

IBM T.J. Watson Research Center, Yorktown Heights, NY 10598

First structural and electrical data are reported for SiGe/Si quantum well structures grown by a new ultra clean low temperature epitaxial deposition process at atmospheric pressure. It is found that the process suppresses the segregation of germanium, possibly by a chemical termination of the surface during the growth. Multiple-quantum-well structures with controllable well widths and abrupt interfaces have been prepared at temperatures ranging from 550 to 650°C. Magneto-transport measurements of modulation doped quantum wells reveal hole mobilities of 2000 cm<sup>2</sup>/Vs at 4.2 K at a carrier density of 1.7\*10<sup>12</sup> cm<sup>-2</sup> and a germanium concentration of 18% in the SiGe channel. Resonant tunneling diodes grown by this technique exhibit well resolved regions of negative differential resistance within a very symmetric I-V characteristic.

**Key words:** Interfaces, resonant tunneling diodes, SiGe quantum wells

## INTRODUCTION

Low temperature epitaxy of SiGe/Si hetero- and quantum well structures has wide applications including bipolar and complementary metal oxide semiconductor (CMOS) technology. The growth of quantum well structures has been implemented by molecular beam epitaxy (MBE),<sup>1,2</sup> ultra-high vacuum chemical vapor deposition (UHV/CVD),<sup>3</sup> and low pressure CVD techniques.<sup>4</sup> Some early work using atmospheric pressure CVD (APCVD) for depositing SiGe/Si multi-layer structures yielded smeared interfaces.<sup>5</sup> The technique used in this work, ultra clean APCVD, is a very versatile process that includes an in-situ preclean of the substrate at moderate temperatures (typically 950°C), temperature flexibility, excellent temperature uniformity, and a simple flow-through design that avoids vacuum pumps. A more detailed description of the tool is reported elsewhere.<sup>6,7</sup> It has been shown previously that this technique is capable of depositing SiGe/Si multi-layer structures.<sup>8</sup> This paper extends that work toward quantum well structures and quantum well devices.

Multiple quantum well structures and superlattices provide excellent opportunities to characterize

an epitaxial system in terms of reproducibility and interface control, since several characterization techniques can be brought to bear, providing insights into the structural properties on a monolayer scale. To date, MBE is the technique that has dominated fabrication of SiGe/Si quantum wells. Superlattices with high structural perfection grown by MBE have been reported.<sup>9</sup> The interface roughness appears to be determined by the germanium segregation, which can be suppressed at very low growth temperatures.<sup>10</sup> SiGe/Si quantum wells deposited above 550°C by CVD techniques at very low pressures typically contain some roughness at the SiGe/Si interfaces,<sup>11</sup> which might be attributed to three-dimensional growth. Ultra-high vacuum chemical vapor deposition at temperatures below 550°C seems to minimize this problem, presumably due to surface hydrogen passivation.<sup>3</sup>

However, these temperatures lead to extremely low growth rates. We study here the capability of APCVD to grow SiGe/Si quantum well structures with abrupt interfaces and controlled well widths in the temperature range of 550 to 650°C.

## EXPERIMENTAL

The SiGe/Si quantum wells were deposited using SiCl<sub>2</sub>H<sub>2</sub> (DCS) and GeH<sub>4</sub> as silicon and germanium

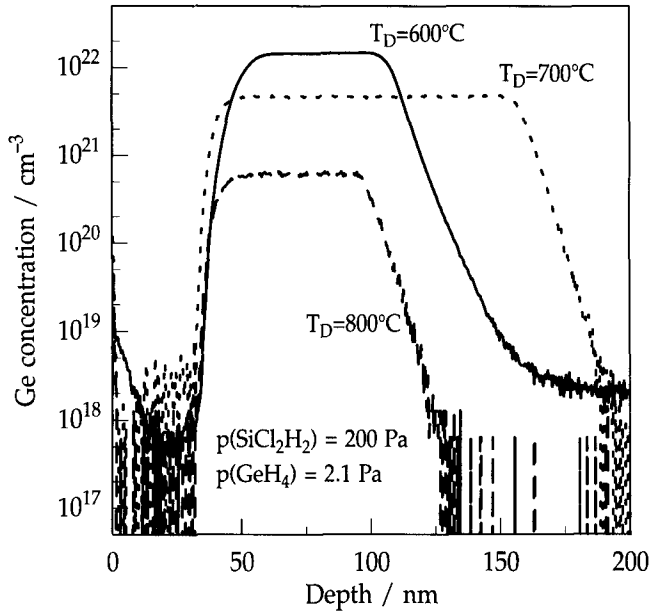


Fig. 1. Secondary ion mass spectrometry profiles of SiGe layers with various germanium contents and thicknesses capped by 40 nm wide silicon top layers, deposited at 600, 700, and 800°C.

sources, respectively, in a  $H_2$  atmosphere at temperatures from 550 to 650°C. The well width was a predictable function of growth time obtained from bulk film growth data. The germanium concentration in the wells was calculated from data obtained from Rutherford backscattering (RBS) on thick films grown under identical conditions. The growth was interrupted at each interface for 20s to switch the gas phase.

The structures were analyzed by high resolution x-ray diffractometry and x-ray reflectivity using a four-crystal diffractometer.<sup>12</sup> Secondary ion mass spectrometry (SIMS) depth profiling measurements were performed with an  $O_2^+$  primary beam with an energy of 2 keV. In addition, the structural properties were investigated by transmission electron microscopy (TEM).

The modulation doped quantum well structures were cleaved into bars for Hall measurements. The ohmic contacts were prepared by evaporating aluminum on the surface followed by an anneal at 550°C for 1 min. The temperature resolved Hall measurements were performed at a magnetic field of 0.44 T and for at least two different currents per sample.

The ohmic contacts of the resonant tunnel diodes (RTD) were formed by Ti/Al metallization, with square top contacts. The contacts served as masks for the subsequent reactive ion etching used to isolate the devices.

## RESULTS AND DISCUSSION

Figure 1 shows the germanium SIMS profiles for three buried SiGe layers of variable thickness grown at 600, 700, and 800°C. In each case, the thick SiGe layer was capped with a 40 nm wide silicon layer. The DCS and  $GeH_4$  partial pressures were kept constant leading to decreasing germanium concentrations in

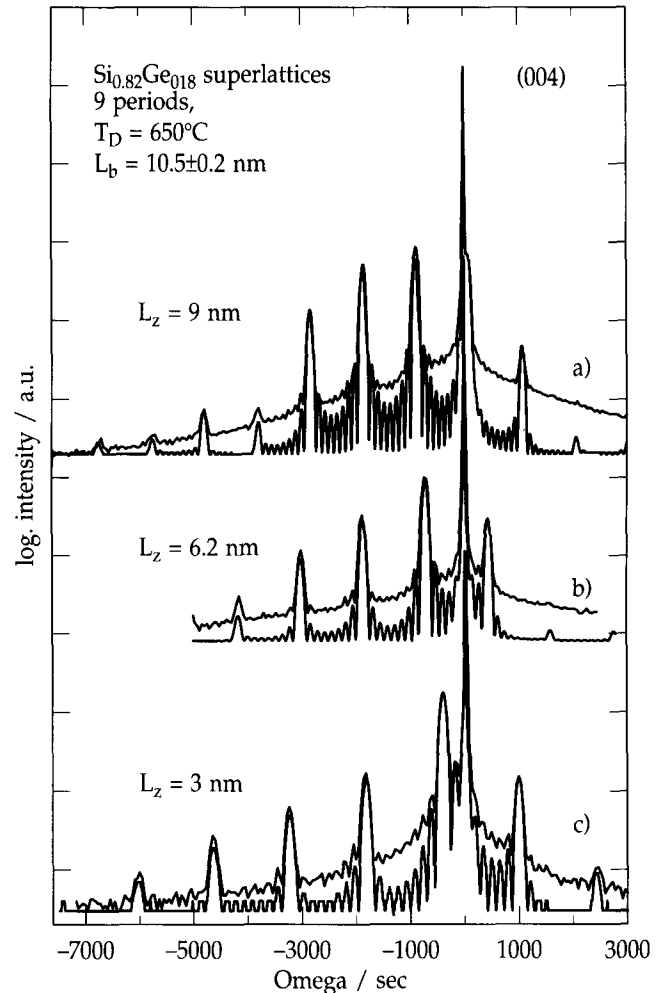


Fig. 2. Measured and modeled x-ray diffraction patterns of SiGe/Si MQWs with 18.3% germanium in the well and nominal well widths of 9, 6, and 3 nm.

the films with increasing temperatures. The important result is that the shape of the germanium profile at the interface between the silicon cap layer and the SiGe layer remains the same, independent of the growth temperature. Even at 800°C, the germanium profile drops three orders of magnitude in 11 nm into the cap layer. The steepness of the profile and the germanium background level ( $< 10^{18} \text{ cm}^{-3}$ ) in the silicon cap are limited by resolution and sensitivity limits of the SIMS. It is remarkable that up to 800°C no indication of germanium segregation (smearing of the germanium profile) is observed. In comparison to MBE data, which show a distinct segregation at temperatures as low as 600°C,<sup>13</sup> this profile sharpness suggests that a mechanism exists in APCVD that impedes germanium segregation. Most likely this is explained by chemical termination of the silicon during the growth in the hydrogen atmosphere. Surface studies of adsorption mechanisms of  $SiCl_2H_2$  on silicon in an UHV chamber show that the surface is covered with SiCl and SiH. Under UHV conditions, the hydrogen is released at 550°C and the chlorine at 730°C from the surface. In the hydrogen atmosphere of the APCVD, the surface appears to be covered with

**Table I. Comparison of Barrier Width, Well Width and Ge Concentration in MQWs Calculated on the Base of RBS Data and Growth Time per Well with Values Determined by Modeling X-Ray Rocking Curves**

Well Growth Time (s)	T (°C)	Calculated MQW Structure			Best Fit MQW Structure from Modeling		
		Barrier (nm)	Well (nm)	Ge (%)	Barrier (nm)	Well (nm)	Ge (%)
60	650	10.5	9.0	18	10.7	9.0	18.3
40	650	10.5	6.0	18	10.5	6.2	18.3
20	650	10.5	3.0	15	10.7	3.0	18.3
100	600	15.0	8.0	29	14.7	8.2	28.5
50	600	15.0	4.0	29	14.7	4.1	28.5
25	600	15.0	2.0	29	14.8	2.0	28.7
120	550	4.0	4.5	39	3.9	4.4	39
80	550	4.0	3.0	39	3.1	3.1	38
40	550	3.0	1.5	39	3.1	1.5	39

hydrogen up to 800°C in dynamic equilibrium with the H<sub>2</sub> in the ambient. This finding is a striking advantage of APCVD. The very sharp germanium transitions also indicate that the island formation and/or the three-dimensional growth are not factors in chemically terminated growth by APCVD. This should lead to smooth interfaces in quantum well structures. A more detailed discussion of the germanium segregation is given elsewhere.<sup>13</sup>

Figure 2 shows the x-ray rocking curves of three SiGe/Si MQW structures, containing nine periods consisting of 10.5 nm wide silicon barriers and 3, 6, and 9 nm wide wells with a germanium concentration of 18%. These well widths were obtained using growth times of 20, 40, and 60 s, respectively, which were calculated from growth data obtained by RBS on bulk samples. The germanium concentration was also determined by RBS on the same bulk samples. In all cases, the best fit of the rocking curve revealed a germanium concentration of 18.3%, and that deviations of more than 0.2 nm of the well and barrier widths were not detected. Similar sets of samples have been deposited at 550 and 600°C with germanium concentrations of 39 and 29%, respectively. The data comparing the best fit and the design values of the multiple-quantum wells (MQWs) are summarized in Table I. In all cases, no discrepancies of more than 1% of germanium or 0.2 nm in well and barrier width were detected. The accuracy of the x-ray diffractometry toward the well and barrier width is of the order of 0.2 nm. For larger variations, the intensities of the high order satellites in the simulated pattern do not fit the experimental data. These data illustrate the precise control of growth available by APCVD.

The sensitivity of the x-ray diffractometry toward interface roughness is illustrated in Fig. 3. Curve 1) in Fig. 3a represents the higher order satellites of the experimentally determined rocking curve of the MQW containing nine periods of 9 nm wide SiGe wells and 10.7 nm thick silicon barriers. The curves 2), 3), and 4) are simulations of the diffraction assuming abrupt interfaces and 1 and 2 nm wide linear gradings of the germanium content at the interfaces, respectively. It

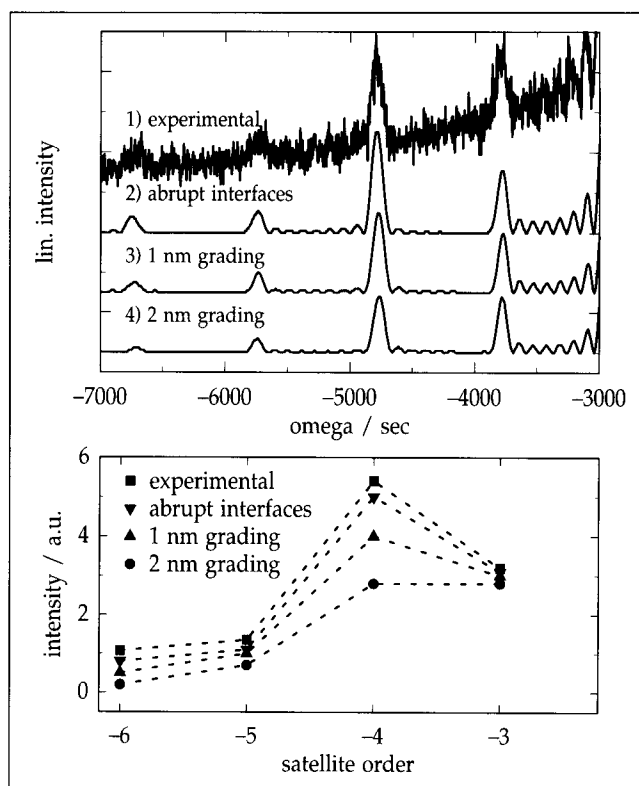


**Fig. 3.** Effect of interface roughness on the intensities of high order satellites for a SiGe/Si MQW containing 9 nm wide wells with a germanium concentration of 18.3% and 10.5 nm wide barriers.

is apparent that the assumption of a smeared interface [Fig. 3a 3), 4)] leads to a reduction of the intensity of the high order satellite peaks. This is shown graphically in Fig. 3b comparing the absolute intensities of the satellites of the simulations with the experimental data after subtracting the background. The best fit is obtained assuming abrupt interfaces. However, due to the noise of the experimental data, a roughness of up to 1 nm at the interfaces cannot be excluded.

A more sensitive method to determine the interface roughness is x-ray reflectivity.<sup>14</sup> Figure 4 depicts the reflection pattern of the same MQW structure as described in Fig 3. Maxima of the reflectivity up to the 14th order are clearly resolved in the pattern. The

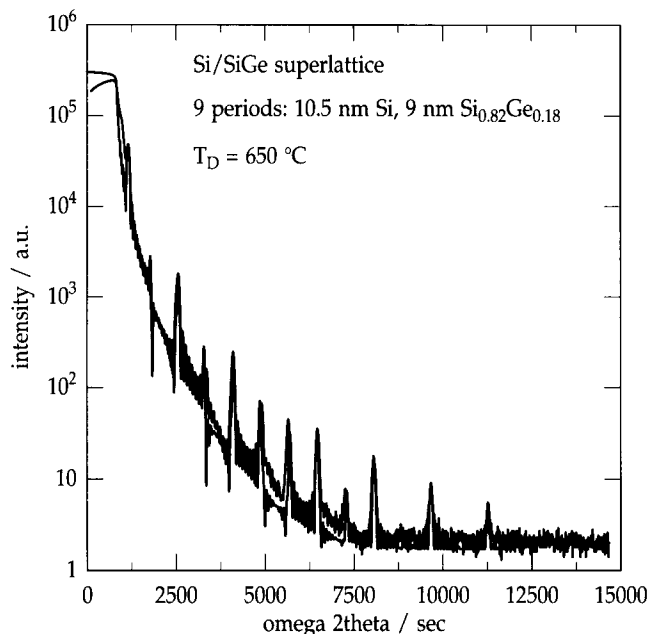


Fig. 4. Comparison of modeled and measured x-ray reflectivity curves.

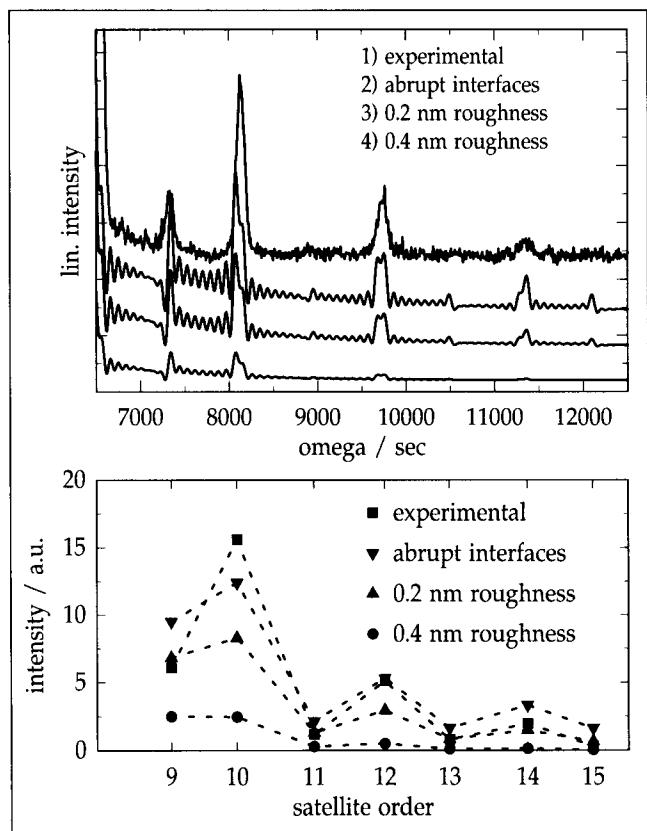


Fig. 5. Effect of interface roughness on the intensities of high order reflectivity peaks.

simulated reflectivity assuming the same germanium concentration and well and barrier width as determined by x-ray diffractometry shows an excellent match with the experimental data. Again, the most sensitive parts of the curve for interface roughness are the higher order maxima. Figure 5 focuses on this part of the pattern. Figure 5a compares the

experimental data 1) with simulations assuming an abrupt interface 2), a roughness of 0.2 nm 3), and a roughness of 0.4 nm 4), at the interfaces. Figure 5b compares the absolute intensities of the reflection maxima for these cases. Clearly, the assumption of an interface roughness of 0.4 nm leads to very weak intensities of the satellites that does not agree with the measured data. From this measurement, we are able to conclude that the interface roughness is about 0.2 nm or less; i.e. in the monolayer range. It is important to point out that the reflectivity is not dependent on whether this roughness is due to a long or a short range fluctuation of the well width or due to a SiGe monolayer at the interface that contains a lower germanium fraction than that of the well. The assumption of small changes in the well width from well to well would lead to a shift of intensity from the satellites into the Pendellösungen, which is not observed in the experimental data.

Transmission electron microscopy cross sections from several MQWs support the findings of the x-ray diffraction and reflection measurements. Smooth interfaces have been obtained for a 20-period superlattice grown at 650°C with 1.1 nm wide SiGe wells containing 37.5% germanium and 3.7 nm thick silicon barriers. No indication of three-dimensional growth was found in the sample despite the relatively high deposition temperature of SiGe layers with 37.5% germanium. This supports the earlier conclusion that the germanium segregation is largely suppressed by chemical termination of the surface.

In comparison to samples grown by low pressure CVD at 625°C,<sup>11</sup> the interface roughness of the MQWs grown by APCVD at 550 to 650°C is reduced, which is attributed to the stabilization of the hydrogen passivation at atmospheric pressure. Furthermore, our data indicate that the interfaces are at least as abrupt as for MQWs grown by UHV/CVD. A strict comparison is difficult since no x-ray reflection data or methods of comparable sensitivity toward the interface roughness has been used to analyze samples grown by CVD techniques at very low pressures. X-ray reflectivity data from MQWs grown by MBE show a short range roughness of 0.5 nm and a long range roughness of 0.9 nm<sup>14</sup> compared to 0.2 nm in the samples grown in this study. In contrast to MBE, the interface abruptness in the MQWs grown by APCVD appears to be determined by the gas switching sequence rather than by germanium segregation. Under the present operating conditions, APCVD is a very powerful technique for the deposition of SiGe/Si quantum well structures and that earlier results showing smeared interfaces in APCVD grown multi-layers<sup>5</sup> can be attributed to high growth temperatures (900–1000°C) and less than optimal gas switching sequences.

Figure 6 shows a TEM cross section of a quantum well structure grown at 550°C. It is designed for resonant tunneling. The SiGe layers appear dark and the silicon layers bright in the TEM image. The structure consists of a 6 nm wide SiGe quantum well

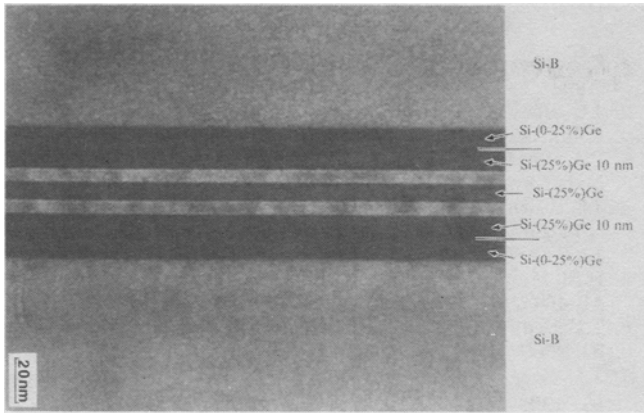


Fig. 6. Cross-sectional TEM of a resonant tunnel structure containing two 5 nm wide silicon barriers and a 6 nm SiGe well.

(25% germanium) with 5 nm thick silicon barriers on either side sandwiched between SiGe layers that contain a 10 nm thick layer of 25% germanium and then the germanium is graded down toward the B-doped silicon top and bottom layers to avoid spikes in the valence band at the top and bottom SiGe interfaces. The TEM reveals smooth interfaces with no indication of undulations or roughness between the SiGe layers and the two silicon barriers.

Figure 7 shows the I-V characteristics of this particular resonant tunneling structure for a  $20 \times 20 \mu\text{m}$  area resonant tunneling diode (RTD) at 4.2 K. Well resolved regions of negative differential resistance have been detected. The I-V curve remains nearly identical up to temperatures of 77 K. At room temperature no regions of negative differential resistance are observed. On either side of the I-V curve, five peaks are resolved that can be attributed to the tunneling via three heavy hole subbands  $\text{HH}_0$ ,  $\text{HH}_1$ , and  $\text{HH}_2$  and two light hole subbands  $\text{LH}_0$  and  $\text{LH}_1$ . An oversimplified calculation assuming a linear interpolation between the silicon and germanium values for the effective masses<sup>15</sup> leads to the subband positions within the valence band of the double barrier structure shown in the inset of Fig. 7. The agreement between the observed and the calculated values is reasonably good. The resonant current peaks were detected at 40, 180, 195, 370, and 420 mV in forward bias and at -50, -145, -180, -315, and -365 mV in reverse bias. The slight asymmetry is probably due to differences in doping levels of the top silicon layer and the silicon substrate. The peak to valley ratio of the features is comparable to those obtained for MBE-grown<sup>16,17</sup> Si/SiGe RTDs, confirming that the APCVD is capable of producing SiGe/Si quantum well structures with abrupt interfaces.

The structural properties are promising for applications of APCVD grown quantum well structures in CMOS devices, since the abrupt interfaces should suppress the interface scattering of two-dimensional (2-D) hole gases. Modulation doped single quantum well structures containing a 8 nm wide SiGe well separated from the B-doped spikes by 4 nm thick silicon undoped silicon spacer layers have been pre-

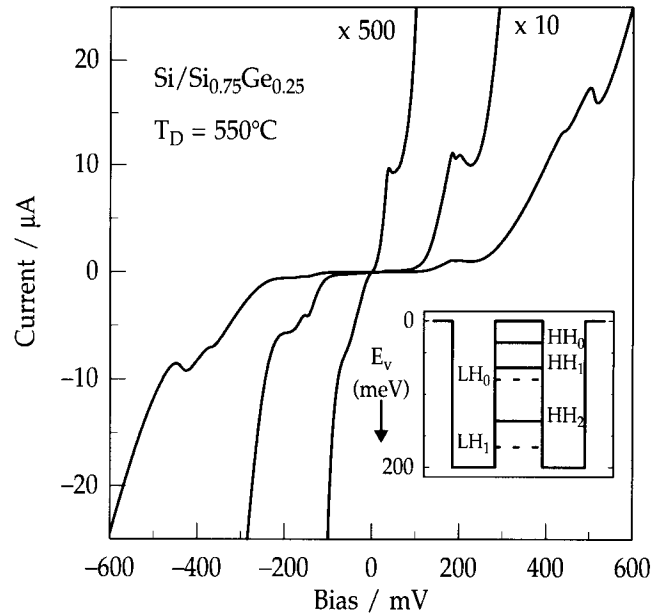


Fig. 7. I-V characteristics of a SiGe/Si resonant tunnel diode.

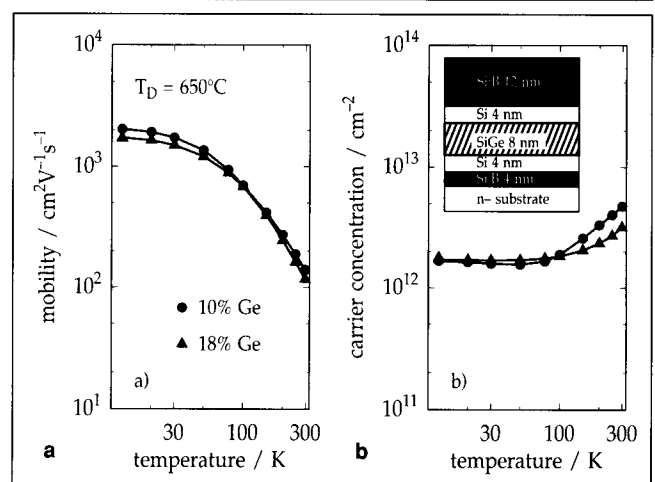


Fig. 8. Temperature dependence of a) Hall mobilities and b) sheet carrier densities of modulation doped SiGe/Si single quantum well structures (inset Fig. 8b).

pared at 650°C. The doping level was  $4 \times 10^{18} \text{ cm}^{-3}$  in the 4 nm wide Si:B layer underneath and the 12 nm thick cap layer. The thicker B-doped layer on the top of the structure was used to saturate the surface states. The structure is outlined in the inset of Fig. 8b. Figures 8a and b show the Hall mobility a) and carrier concentration b) in dependence on the temperature for modulation doped single quantum wells with 10 and 18% germanium in the well. Both samples show the expected temperature dependence of a 2-D hole gas. The mobility and the carrier concentration of the sample containing 10% germanium in the channel is slightly higher than that of the sample with 18%, peaking to 2035  $\text{cm}^2/\text{Vs}$  at a sheet carrier density of  $1.7 \times 10^{12} \text{ cm}^{-2}$  at 4.2 K. The room temperature mobilities are 135 and 115 at sheet carrier densities of  $5 \times 10^{12}$  and  $3.5 \times 10^{12} \text{ cm}^{-2}$  for 10 and 18% germanium in the well, respectively. Those values are comparable to data published for similar structures.<sup>18</sup> However, no

improvement of the mobilities is observed, which might indicate that interface roughness is not the fundamental limiting scattering mechanism in these samples. Furthermore the increase of the germanium concentration did not lead to higher mobilities, in contradiction to model calculations.<sup>19</sup> It is not believed that background doping limits the mobility since capacitance voltage measurements of thick silicon samples grown under comparable conditions reveal unintentional low doping levels of  $1\text{--}5 \times 10^{14} \text{ cm}^{-3}$ . Other scattering mechanisms that might occur are intersubband scattering, alloy scattering, or scattering at potential fluctuations due to lateral fluctuations of the germanium concentration. However, a more detailed investigation is required.

### CONCLUSIONS

We have employed the deposition of SiGe/Si quantum well structures and superlattices by APCVD. The SIMS, x-ray, and TEM data strongly indicate that germanium segregation does not occur in the temperature range under investigation, which we attribute to the stable chemical termination of the surface due to the hydrogen atmosphere. Consequently, APCVD permits the growth of MQWs with an interface roughness in the monolayer scale. The roughness is determined by the accuracy of the gas switching sequence rather than by germanium segregation. The exact control of well width and germanium concentration suggest that the APCVD is a powerful contender for the growth of quantum devices. The first demonstrations of p-type RTDs with well resolved regions of negative differential resistance as well as 2-D hole gas confinement layers with high mobilities in modulation doped quantum wells illustrates the broad capabilities of the APCVD technique for the deposition of sophisticated device structures with high performances.

### REFERENCES

1. E. Kasper and F. Schäffler, *Semicond. and Semimetals* 33, 223 (1991).
2. J.C. Bean, L.C. Feldman, A.T. Fiory, S. Nakahara and I.K. Robinson, *J. Vac. Sci. Technol. A* 2, 436 (1984).
3. P.J. Wang, M.S. Goorsky, B.S. Meyerson, F.K. LeGoues and M.J. Tejwani, *Appl. Phys. Lett.* 59, 814 (1991).
4. J.C. Sturm, H. Manoharan, L.C. Lenchyshyn, M.L.W. Thewalt, N.L. Rowell, J.P. Noël and D.C. Houghton, *Phys. Rev. Lett.* 66, 1362 (1991).
5. H.M. Manasevit, I.S. Gergis and A.B. Jones, *Appl. Phys. Lett.* 41, 464 (1982).
6. T.O. Sedgwick, M. Berkenblit and T.S. Kuan, *Appl. Phys. Lett.* 54, 2689 (1989).
7. T.O. Sedgwick, V.P. Kesan, P.D. Agnello, D.A. Grützmaker, D. Nguyen-Ngoc, S.S. Iyer, D.J. Meyer and A.P. Ferro, *Proc. of IEDM 1991*, Washington D.C., p. 451
8. P. Agnello, T.O. Sedgwick, M.S. Goorsky, J. Ott, T.S. Kuan and G. Scilla, *Appl. Phys. Lett.* 59, 1479 (1991).
9. K. Eberl, W. Wegscheider, R. Schorer and G. Abstreiter, *Phys. Rev. B* 43, 5188 (1991).
10. D.J. Gravesteijn, P.C. Zalm, G.F.A. van de Walle, C.J. Vriezema A.A. van Gorkum and L.J. Ijzendoorn, *Thin Solid Films* 183, 191 (1989).
11. X. Xiao, C.W. Liu, J.C. Sturm, L.C. Lenchyshyn, M.L.W. Thewalt, R.B. Gregory and P. Fejes, *Appl. Phys. Lett.* 60, 2135 (1992).
12. D.A. Grützmaker and T.O. Sedgwick, to be published.
13. D.A. Grützmaker, A. Powell, M. Tejwani, T.O. Sedgwick, S.S. Iyer and J. Cotte, *Appl. Phys. Lett.* 61, 2872 (1992).
14. A.R. Powell, D.K. Bowen, M. Wormington, R.A. Kubiak, E.H.C. Parker, J. Hudson and P.D. Augustus, *Semicond. Sci. Technol.* 7, 627 (1992).
15. A. Zaslavsky, D.A. Grützmaker, Y.H. Lee, W. Ziegler and T.O. Sedgwick, *Appl. Phys. Lett.* 61, 2872 (1992).
16. K.L. Wang, R.P. Karunasiri, J. Park, S.S. Rhee and C.H. Chern, *Superlatt. Microstruct.* 5, 201 (1989).
17. U. Gennser, V.P. Kesan, S.S. Iyer, T.J. Brucelot and E.S. Yang, *J. Vac. Sci. Technol.* B8, 210 (1990).
18. P.J. Wang, B.S. Meyerson, F.F. Fang, J. Nocera and B. Parker, *Appl. Phys. Lett.* 55, 2333 (1989).
19. T. Manku and A. Nathan, *IEEE Electron Dev. Lett.* 12, 704 (1991).